Supplemental Materials for

The NOX4 pathway as a source of selective insulin resistance and responsiveness

Xiangdong Wu and Kevin Jon Williams

From the Section of Endocrinology, Diabetes, and Metabolism, Department of Medicine (XW & KJW) and the Cardiovascular Research Center, Department of Physiology (KJW), Temple University School of Medicine, Philadelphia, PA USA.

Correspondence to:
Kevin Jon Williams, M.D.
Professor of Medicine
Chief, Section of Endocrinology, Diabetes, & Metabolism
Temple University School of Medicine
3322 North Broad Street
Medical Office Building, Room 212
Philadelphia, PA 19140 USA
Tel.: (215)707-4746; FAX: (215)707-5599
eMAIL: kjwilliams@temple.edu.

Supplemental Background

Prior literature has documented major site-specific phosphorylations and functions in the AKT limb of insulin receptor signaling (see Figure 1). Insulin-stimulated phosphorylation of FOXO1 has been reported at Thr24, a key site normally phosphorylated by activated AKT, leading to exclusion of FOXO1 from the nucleus[1] and arresting its activity as a transcription factor for apoC-III and gluconeogenic genes.[2-5]

The AKT limb also affects several molecules involved in lipogenesis. The AKT target site on glycogen synthase kinase-3ß (GSK3ß) is Ser9.[6] Phosphorylation by AKT inactivates GSK3,[6] and may thereby block this factor from inhibiting ACL, a key enzyme in fatty acid, cholesterol, and new glucose biosynthesis,[7, 8] as well as glycogen synthase. Insulin induces activation and site-specific serine-phosphorylation of a second enzyme in fatty acid biosynthesis, acetyl-CoA carboxylase-1 (ACC).[9, 10] The effect of phosphorylation of ACC at Ser79 on its activity in vitro remains an open question,[11] whereas in vivo, T2DM increases hepatic ACC activity and Ser79-phosphorylation together.[12] We infer that overphosphorylation at Ser79 in T2DM liver in vivo could be driven by hyperinsulinemia in combination with continued responsiveness of this portion of the insulin receptor-AKT signaling cascade.

Another lipogenic target of AKT is the mammalian target of rapamycin complex-1 (mTORC1), which is activated in the tissues of obese mice.[13, 14] This complex has two AKT-dependent inputs: PRAS40[15] and TSC2.[16, 17] Insulin stimulates AKT to phosphorylate PRAS40[15, 18] at Thr246.[19] Insulin-stimulated phosphorylation of TSC2 occurs at a key site acted on by AKT, Thr1462.[20] Insulin-induced mTORC1 activity can be assess by the phosphorylation of one of its substrates – namely, the ribosomal protein S6 kinase 1 (S6K1), an enzyme that desensitizes IRS1 in states of overnutrition and obesity (reference[21] and Figure 1). Activated mTORC1 induces *Srebp1c* mRNA, which encodes a major insulin-responsive transcription factor in lipogenesis.[22-26] Activated mTORC1 might also increase lipogenesis through induction of ER stress[17] and hence

cleavage and activation of the SREBP1c protein.[27, 28] All of these effects are displayed schematically in Figure 1.

Pathways of interest that are not in Figure 1 include suppression of *Irs2* mRNA by insulin;[29] insulin-induced activation of mitogen-activated protein kinases in addition to ERK1,2;[30] our sequence analysis of NOX4 and subsequent inference that NOX4 in cholesterol-rich caveolae could contribute to the putative generation of oxysterol ligands for LXR after insulin stimulation (Methods); inhibition of GLUT translocation by activated mTORC1;[31] insulin-stimulated production of the vasodilator NO via activated AKT and of the vasoconstrictor endothelin-1 via activated ERK;[32] direct effects of activated PI3K on ER stress;[33, 34] insulin-stimulated phosphorylation and inhibition of FOXA2, a transcriptional factor that otherwise drives the expression of genes encoding enzymes of fatty acid oxidation, ketogenesis, and glycolysis;[35] insulin-induced cleavage and activation of SREBP1c protein via PI3K;[36] ERK-mediated phosphorylation of SREBP1c at Ser93, which enhances transactivation of its target genes;[37-39] the ability of activated MEK to bind, inhibit, and provoke the expulsion of PPARγ from the nucleus;[40, 41] and effects of insulin on sympathetic activity,[42, 43] renal sodium excretion,[42, 44-46] ERK-mediated phosphorylation and activation of the Na^+/K^+ ATPase,[47] coagulation,[48-50] expression of matrix metalloproteinases,[30] and secretion of apoB-containing lipoproteins.[5, 51-54]

Supplemental References

1. Biggs WH, 3rd, Meisenhelder J, Hunter T, Cavenee WK, Arden KC. Protein kinase B/Akt-mediated phosphorylation promotes nuclear exclusion of the winged helix transcription factor FKHR1. *Proc Natl Acad Sci U S A.* 1999;96:7421-7426.
2. Hall RK, Yamasaki T, Kucera T, Waltner-Law M, O'Brien R, Granner DK. Regulation of phosphoenolpyruvate carboxykinase and insulin-like growth factor-binding protein-1 gene expression by insulin. The role of winged helix/forkhead proteins. *J Biol Chem.* 2000;275:30169-30175.
3. Puigserver P, Rhee J, Donovan J, Walkey CJ, Yoon JC, Oriente F, Kitamura Y, Altomonte J, Dong H, Accili D, Spiegelman BM. Insulin-regulated hepatic gluconeogenesis through FOXO1-PGC-1α interaction. *Nature.* 2003;423:550-555.
4. Altomonte J, Cong L, Harbaran S, Richter A, Xu J, Meseck M, Dong HH. Foxo1 mediates insulin action on apoC-III and triglyceride metabolism. *J Clin Invest.* 2004;114:1493-1503.
5. Sparks JD, Dong HH. FoxO1 and hepatic lipid metabolism. *Curr Opin Lipidol.* 2009;20:217-226.
6. Cross DA, Alessi DR, Cohen P, Andjelkovich M, Hemmings BA. Inhibition of glycogen synthase kinase-3 by insulin mediated by protein kinase B. *Nature.* 1995;378:785-789.
7. Hughes K, Ramakrishna S, Benjamin WB, Woodgett JR. Identification of multifunctional ATP-citrate lyase kinase as the α-isoform of glycogen synthase kinase-3. *Biochem J.* 1992;288 (Pt 1):309-314.
8. Potapova IA, El-Maghrabi MR, Doronin SV, Benjamin WB. Phosphorylation of recombinant human ATP:citrate lyase by cAMP-dependent protein kinase abolishes homotropic allosteric regulation of the enzyme by citrate and increases the enzyme activity. Allosteric activation of ATP:citrate lyase by phosphorylated sugars. *Biochemistry.* 2000;39:1169-1179.

9. Witters LA, Tipper JP, Bacon GW. Stimulation of site-specific phosphorylation of acetyl coenzyme A carboxylase by insulin and epinephrine. *J Biol Chem.* 1983;258:5643-5648.
10. Heesom KJ, Moule SK, Denton RM. Purification and characterisation of an insulin-stimulated protein-serine kinase which phosphorylates acetyl-CoA carboxylase. *FEBS Lett.* 1998;422:43-46.
11. Munday MR. Regulation of mammalian acetyl-CoA carboxylase. *Biochem Soc Trans.* 2002;30:1059-1064.
12. Ouadda ABD, Levy E, Ziv E, Lalonde G, Sane AT, Delvin E, Elchebly M. Increased hepatic lipogenesis in insulin resistance and type 2 diabetes is associated with AMPK signalling pathway up-regulation in *Psammomys obesus*. *Biosci Rep.* 2009;29:283-292.
13. Um SH, Frigerio F, Watanabe M, Picard F, Joaquin M, Sticker M, Fumagalli S, Allegrini PR, Kozma SC, Auwerx J, Thomas G. Absence of S6K1 protects against age- and diet-induced obesity while enhancing insulin sensitivity. *Nature.* 2004;431:200-205.
14. Khamzina L, Veilleux A, Bergeron S, Marette A. Increased activation of the mammalian target of rapamycin pathway in liver and skeletal muscle of obese rats: possible involvement in obesity-linked insulin resistance. *Endocrinology.* 2005;146:1473-1481.
15. Sancak Y, Thoreen CC, Peterson TR, Lindquist RA, Kang SA, Spooner E, Carr SA, Sabatini DM. PRAS40 is an insulin-regulated inhibitor of the mTORC1 protein kinase. *Mol Cell.* 2007;25:903-915.
16. Tee AR, Fingar DC, Manning BD, Kwiatkowski DJ, Cantley LC, Blenis J. Tuberous sclerosis complex-1 and -2 gene products function together to inhibit mammalian target of rapamycin (mTOR)-mediated downstream signaling. *Proc Natl Acad Sci U S A.* 2002;99:13571-13576.
17. Ozcan U, Ozcan L, Yilmaz E, Duvel K, Sahin M, Manning BD, Hotamisligil GS. Loss of the tuberous sclerosis complex tumor suppressors triggers the unfolded protein response to regulate insulin signaling and apoptosis. *Mol Cell.* 2008;29:541-551.

18. Vander Haar E, Lee SI, Bandhakavi S, Griffin TJ, Kim DH. Insulin signalling to mTOR mediated by the Akt/PKB substrate PRAS40. *Nat Cell Biol.* 2007;9:316-323.
19. Wang L, Harris TE, Lawrence JC, Jr. Regulation of proline-rich Akt substrate of 40 kDa (PRAS40) function by mammalian target of rapamycin complex 1 (mTORC1)-mediated phosphorylation. *J Biol Chem.* 2008;283:15619-15627.
20. Manning BD, Cantley LC. United at last: the tuberous sclerosis complex gene products connect the phosphoinositide 3-kinase/Akt pathway to mammalian target of rapamycin (mTOR) signalling. *Biochem Soc Trans.* 2003;31:573-578.
21. Tremblay F, Brule S, Hee Um S, Li Y, Masuda K, Roden M, Sun XJ, Krebs M, Polakiewicz RD, Thomas G, Marette A. Identification of IRS-1 Ser-1101 as a target of S6K1 in nutrient- and obesity-induced insulin resistance. *Proc Natl Acad Sci U S A.* 2007;104:14056-14061.
22. Tontonoz P, Kim JB, Graves RA, Spiegelman BM. ADD1: a novel helix-loop-helix transcription factor associated with adipocyte determination and differentiation. *Mol Cell Biol.* 1993;13:4753-4759.
23. Foretz M, Pacot C, Dugail I, Lemarchand P, Guichard C, Le Lièpvre X, Berthelier-Lubrano C, Spiegelman B, Kim JB, Ferré P, Foufelle F. ADD1/SREBP-1c is required in the activation of hepatic lipogenic gene expression by glucose. *Mol Cell Biol.* 1999;19:3760-3768.
24. Horton JD, Goldstein JL, Brown MS. SREBPs: activators of the complete program of cholesterol and fatty acid synthesis in the liver. *J Clin Invest.* 2002;109:1125-1131.
25. Leavens KF, Easton RM, Shulman GI, Previs SF, Birnbaum MJ. Akt2 is required for hepatic lipid accumulation in models of insulin resistance. *Cell Metab.* 2009;10:405-418.
26. Li S, Brown MS, Goldstein JL. Bifurcation of insulin signaling pathway in rat liver: mTORC1 required for stimulation of lipogenesis, but not inhibition of gluconeogenesis. *Proc Natl Acad Sci U S A.* 2010;107:3441-3446.

27. Kammoun HL, Chabanon H, Hainault I, Luquet S, Magnan C, Koike T, Ferré P, Foufelle F. GRP78 expression inhibits insulin and ER stress-induced SREBP-1c activation and reduces hepatic steatosis in mice. *J Clin Invest.* 2009;119:1201-1215.
28. Laplante M, Sabatini DM. mTORC1 activates SREBP-1c and uncouples lipogenesis from gluconeogenesis. *Proc Natl Acad Sci U S A.* 2010;107:3281-3282.
29. Zhang J, Ou J, Bashmakov Y, Horton JD, Brown MS, Goldstein JL. Insulin inhibits transcription of IRS-2 gene in rat liver through an insulin response element (IRE) that resembles IREs of other insulin-repressed genes. *Proc Natl Acad Sci U S A.* 2001;98:3756-3761.
30. Boden G, Song W, Pashko L, Kresge K. In vivo effects of insulin and free fatty acids on matrix metalloproteinases in rat aorta. *Diabetes.* 2008;57:476-483.
31. Jiang X, Kenerson H, Aicher L, Miyaoka R, Eary J, Bissler J, Yeung RS. The tuberous sclerosis complex regulates trafficking of glucose transporters and glucose uptake. *Am J Pathol.* 2008;172:1748-1756.
32. Muniyappa R, Montagnani M, Koh KK, Quon MJ. Cardiovascular actions of insulin. *Endocr Rev.* 2007;28:463-491.
33. Park SW, Zhou Y, Lee J, Lu A, Sun C, Chung J, Ueki K, Ozcan U. The regulatory subunits of PI3K, p85α and p85ß, interact with XBP-1 and increase its nuclear translocation. *Nat Med.* 2010;16:429-437.
34. Winnay JN, Boucher J, Mori MA, Ueki K, Kahn CR. A regulatory subunit of phosphoinositide 3-kinase increases the nuclear accumulation of X-box-binding protein-1 to modulate the unfolded protein response. *Nat Med.* 2010;16:438-445.
35. Wolfrum C, Asilmaz E, Luca E, Friedman JM, Stoffel M. Foxa2 regulates lipid metabolism and ketogenesis in the liver during fasting and in diabetes. *Nature.* 2004;432:1027-1032.
36. Hegarty BD, Bobard A, Hainault I, Ferré P, Bossard P, Foufelle F. Distinct roles of insulin and liver X receptor in the induction and cleavage of sterol

regulatory element-binding protein-1c. *Proc Natl Acad Sci U S A.* 2005;102:791-796.

37. Kotzka J, Muller-Wieland D, Koponen A, Njamen D, Kremer L, Roth G, Munck M, Knebel B, Krone W. ADD1/SREBP-1c mediates insulin-induced gene expression linked to the MAP kinase pathway. *Biochem Biophys Res Commun.* 1998;249:375-379.
38. Arito M, Horiba T, Hachimura S, Inoue J, Sato R. Growth factor-induced phosphorylation of sterol regulatory element-binding proteins inhibits sumoylation, thereby stimulating the expression of their target genes, low density lipoprotein uptake, and lipid synthesis. *J Biol Chem.* 2008;283:15224-15231.
39. Müller-Wieland D, Knebel B, Haas J, Kotzka J. SREBPs and fatty liver: relevance for obesity, diabetes, dyslipidemia and atherosclerosis. *XVII Lipid Meeting Leipzig.* 2011; http://www.lipidmeeting.de/program.php.
40. Burgermeister E, Chuderland D, Hanoch T, Meyer M, Liscovitch M, Seger R. Interaction with MEK causes nuclear export and downregulation of peroxisome proliferator-activated receptor γ. *Mol Cell Biol.* 2007;27:803-817.
41. Khateeb J, Kiyan Y, Aviram M, Tkachuk S, Dumler I, Fuhrman B. Urokinase-type plasminogen activator downregulates paraoxonase 1 expression in hepatocytes by stimulating peroxisome proliferator–activated receptor-γ nuclear export *Arterioscler Thromb Vasc Biol.* doi:10.1161/ATVBAHA.111.239889; ePub: 8 Dec 2011.
42. Brands MW, Lee WF, Keen HL, Alonso-Galicia M, Zappe DH, Hall JE. Cardiac output and renal function during insulin hypertension in Sprague-Dawley rats. *Am J Physiol.* 1996;271:R276-281.
43. Ward KR, Bardgett JF, Wolfgang L, Stocker SD. Sympathetic response to insulin is mediated by melanocortin 3/4 receptors in the hypothalamic paraventricular nucleus. *Hypertension.* 2011;57:435-441.
44. Atchley DW, Loeb RF, Richards DW, Benedict EM, Driscoll ME. On diabetic acidosis: A detailed study of electrolyte balances following the

withdrawal and reestablishment of insulin therapy. *J Clin Invest.* 1933;12:297-326.

45. Miller JH, Bogdonoff MD. Antidiuresis associated with administration of insulin. *J Appl Physiol.* 1954;6:509-512.
46. DeFronzo RA, Cooke CR, Andres R, Faloona GR, Davis PJ. The effect of insulin on renal handling of sodium, potassium, calcium, and phosphate in man. *J Clin Invest.* 1975;55:845-855.
47. Al-Khalili L, Kotova O, Tsuchida H, Ehrén I, Féraille E, Krook A, Chibalin AV. ERK1/2 mediates insulin stimulation of Na,K-ATPase by phosphorylation of the α-subunit in human skeletal muscle cells. *J Biol Chem.* 2004;279:25211-25218.
48. Guha M, O'Connell MA, Pawlinski R, Hollis A, McGovern P, Yan SF, Stern D, Mackman N. Lipopolysaccharide activation of the MEK-ERK1/2 pathway in human monocytic cells mediates tissue factor and tumor necrosis factor α expression by inducing Elk-1 phosphorylation and Egr-1 expression. *Blood.* 2001;98:1429-1439.
49. Boden G, Vaidyula VR, Homko C, Cheung P, Rao AK. Circulating tissue factor procoagulant activity and thrombin generation in patients with type 2 diabetes: effects of insulin and glucose. *J Clin Endocrinol Metab.* 2007;92:4352-4358.
50. Li M, Yu D, Williams KJ, Liu ML. Tobacco smoke induces the generation of procoagulant microvesicles from human monocytes/macrophages. *Arterioscler Thromb Vasc Biol.* 2010;30:1818-1824.
51. Taghibiglou C, Carpentier A, Van Iderstine SC, Chen B, Rudy D, Aiton A, Lewis GF, Adeli K. Mechanisms of hepatic very low density lipoprotein overproduction in insulin resistance. Evidence for enhanced lipoprotein assembly, reduced intracellular apoB degradation, and increased microsomal triglyceride transfer protein in a fructose-fed hamster model. *J Biol Chem.* 2000;275:8416-8425.

52. Fisher EA, Williams KJ. Autophagy of an oxidized, aggregated protein beyond the ER: a pathway for remarkably late-stage quality control. *Autophagy.* 2008;4:721-723.
53. Adiels M, Olofsson S-O, Taskinen M-R, Borén J. Overproduction of very low-density lipoproteins is the hallmark of the dyslipidemia in the metabolic syndrome. *Arterioscler Thromb Vasc Biol.* 2008;28:1225-1236.
54. Taskinen MR, Adiels M, Westerbacka J, Söderlund S, Kahri J, Lundbom N, Lundbom J, Hakkarainen A, Olofsson SO, Orho-Melander M, Borén J. Dual metabolic defects are required to produce hypertriglyceridemia in obese subjects. *Arterioscler Thromb Vasc Biol.* 2011;31:2144-2150.

Supplemental figure legends

Supplemental Figure I: Type 2 diabetes renders the liver unable to inactivate PTP1B in response to insulin.
Displayed are PTP1B activities from the same liver samples as in Figure 2, which were obtained just before (*Pre*) and 10min after (*Post*) an intravenous injection of insulin into lean *db/m* mice (controls) and their hyperphagic, obese T2DM *db/db* littermates, as indicated. PTP1B activities in liver homogenates were assayed under strictly anaerobic conditions (mean±SEM, n=3). Statistical comparisons by the paired *t*-test are indicated.

Supplemental Figure II: Type 2 diabetes impairs a key insulin-stimulated hypolipidemic and hypoglycemic pathway in liver, yet preserves lipogenic pathways and robust ERK activation.
Displayed are immunoblots from the same liver samples as in Figure 2, which were obtained just before (*Pre*) and 10min after (*Post*) an intravenous injection of insulin into lean *db/m* mice (controls) and their hyperphagic, obese T2DM *db/db* littermates, as indicated. Panel A: Resistance of FOXO1 to insulin-stimulated phosphorylation in T2DM *db/db* livers compared to control *db/m* livers (*TG-rich lipoprotein clearance* and *Gluconeogenesis* pathways from Figure 1), yet continued responsiveness of GSK3ß (*Lipogenesis-I* pathway from Figure 1). Panel B: Continued activation of molecules upstream (PRAS40) and downstream (S6K1) of mTORC1 in T2DM *db/db* livers (*Lipogenesis-D* pathway from Figure 1). The 70-kDa isoform of S6K1 is indicated. Panel C: Continued responsiveness of ERK to insulin-stimulated phosphorylations in T2DM *db/db* livers (*pT202-ERK*, *pY204-ERK*). Immunoblots for total (*t*-, meaning phosphorylated plus unphosphorylated) amounts of each target protein are shown for each sample. Numbers over the lanes refer to individual animals.

Supplemental Figure III: Inhibition of NOX4 in primary rat hepatocytes impairs the ability of insulin to suppress *Irs2* mRNA levels. Displayed are mRNA quantifications from the same set of cultured hepatocytes as in Figure 5A-C. As indicated, primary rat hepatocytes were pretreated with 0 (vehicle) or 1.0 μM DPI (an inhibitor of NOX4), exposed to 0 or 10nM insulin for 6 h, and then harvested. Displayed are *Irs2* mRNA levels normalized to *ß-actin* mRNA levels (ΔCt) and then expressed relative to the mean value from the cells that had been incubated with neither DPI nor insulin ($2^{-\Delta\Delta Ct}$; mean±SEM, n=4). P<0.001 by ANOVA; columns labeled with different lowercase letters (a, b, c) are statistically different by the Student-Newman-Keuls test (P<0.01).

Supplemental Table I: Antibodies against target proteins.

Target Protein	Epitope	Supplier/ Catalog Number	Description	Molecular weight of target protein
ACC	p-ACC	Cell Signaling #3661	Rabbit polyclonal antibody (Ab) against acetyl-CoA carboxylase that is phosphorylated at Ser79	280 kDa
	t-ACC	Cell Signaling #3676	Rabbit monoclonal antibody (mAb) against total acetyl-CoA carboxylase (phosphorylated and non-phosphorylated)	280 kDa
AKT	pT308-AKT	Cell Signaling #4056	Rabbit mAb against AKT phosphorylated at Thr308	60 kDa
	pS473-AKT	Cell Signaling #4051	Mouse mAb against AKT phosphorylated at Ser473	60 kDa
	t-AKT	Cell Signaling #2920	Mouse mAb against total AKT (phosphorylated and non-phosphorylated; clone 40D4)	60 kDa
ß-actin	ß-actin	Cell Signaling #3700	Mouse mAb against ß-actin	45 kDa
ERK	pT202-ERK	Cell Signaling #4376	Rabbit mAb against Erk1/2 that is phosphorylated at Thr202, regardless of the status of Tyr204	42, 44 kDa
	pY204-ERK	Cell Signaling #4377	Rabbit mAb against Erk1/2 that is phosphorylated at Tyr204, regardless of the status of Thr202	42, 44 kDa
	t-ERK	Cell Signaling #4695	Rabbit mAb against total ERK1/2, also known as the P44/42 mitogen-activated protein kinase	42, 44 kDa
FOXO1	t-FOXO1	Cell Signaling #9454	Rabbit polyclonal Ab against total FOXO1 (used here for immunoprecipitation)	78 to 82 kDa
	pT24-FOXO1	Cell Signaling #9464	Rabbit polyclonal Ab against FOXO1 phosphorylated at Thr24 or FOXO3A phosphorylated at Thr32	78 to 82, 95 kDa
	t-FOXO1	Cell Signaling #2880	Rabbit mAb against total FOXO1 (used here for immunoblotting)	78 to 82 kDa
GSK3ß	pS9-GSK3ß	Cell Signaling #9322	Rabbit mAb against GSK3ß phosphorylated at Ser9	46 kDa
	t-GSK3ß	Cell Signaling #9315	Rabbit mAb against total GSK3ß	46 kDa
NOX4	NOX4	LifeSpan Biosciences #LS-C33986	Rabbit polyclonal Ab against NOX4	67 kDa (isoform 1) 31.8 kDa (isoform 4)
PRAS40	pT246-PRAS40	Cell Signaling #2997	Rabbit mAb against PRAS40 phosphorylated at Thr246	40 kDa
	t-PRAS40	Cell Signaling #2691	Rabbit mAb against total PRAS40	40 kDa
PTEN	PTEN	Cell Signaling #9188	Rabbit mAb against PTEN (used here for immunoprecipitation)	54KDa
	PTEN	Cell Signaling #9556	Mouse mAb against PTEN (used here for immunoblotting)	54KDa
PTP1B	PTP1B	Santa Cruz sc-1718	Goat polyclonal Ab against PTP1B (used here for immunoprecipitation)	50KDa
	PTP1B	Santa Cruz sc-1718-R	Rabbit polyclonal Ab against PTP1B (used here for immunoblotting)	50KDa
S6K1	pT389-S6K1 (70-kDa isoform)	Cell Signaling #9206	Mouse mAb against the 70-kDa isoform of S6 kinase-1 that is phosphorylated at Thr389	70, 85 kDa
	t-S6K1	Cell Signaling #2708	Rabbit mAb against total S6K1	70, 85 kDa
SULF2	SULF2	Santa Cruz sc-68436 (Lot # C1909)	Rabbit polyclonal Ab against SULF2	72 kDa
TSC2	pT1462-TSC2	Cell Signaling #3617	Rabbit mAb against TSC2 (tuberin) phosphorylated at Thr1462	200 kDa
	t-TSC2	Cell Signaling #4308	Rabbit mAb against total TSC2	200 kDa

Supplemental Table II: Primer and probe sequences for quantitative real-time PCR.

Target mRNA	Forward primer	Reverse primer	Probe
Apoc3	5'-atg cag ggc tac atg gaa ca-3'	5'-cac agc tat atc aga ctc ct-3'	F-5'-tcc aag acg gtc cag gat gca ct-3'-Q
Irs2	5'-atg aac ctg gac ttc agt tct-3'	5'-atc cat gga gcc tac tgt gt-3'	F-5'-tcc ccc aag cct agc acc cgc-3'-Q
Pepck	5'-agt cac cat cac ttc ctg ga-3'	5'-cag aat cgc gag ttg gga tg-3'	F-5'-cg gtt cct cat cct gtg gtc tcc ac-3'-Q
Srebp1c	5'-gga gcc atg gat tgc aca tt-3'	5'-cat caa ata ggc cag gga ag-3'	F-5'-tg ctt cag ctc atc aac aac caa gac a-3'-Q
ß-actin	5'-tgc ctg acg gtc agg tca-3'	5'-cag gaa gga agg ctg gaa g-3'	F-5'-ca cta tcg gca atg agc ggt tcc g-3'-Q

In the probe sequences, *F* and *Q* denote the positions of the FAM fluorophore and TAMRA quencher, respectively.

Supplemental Figure I

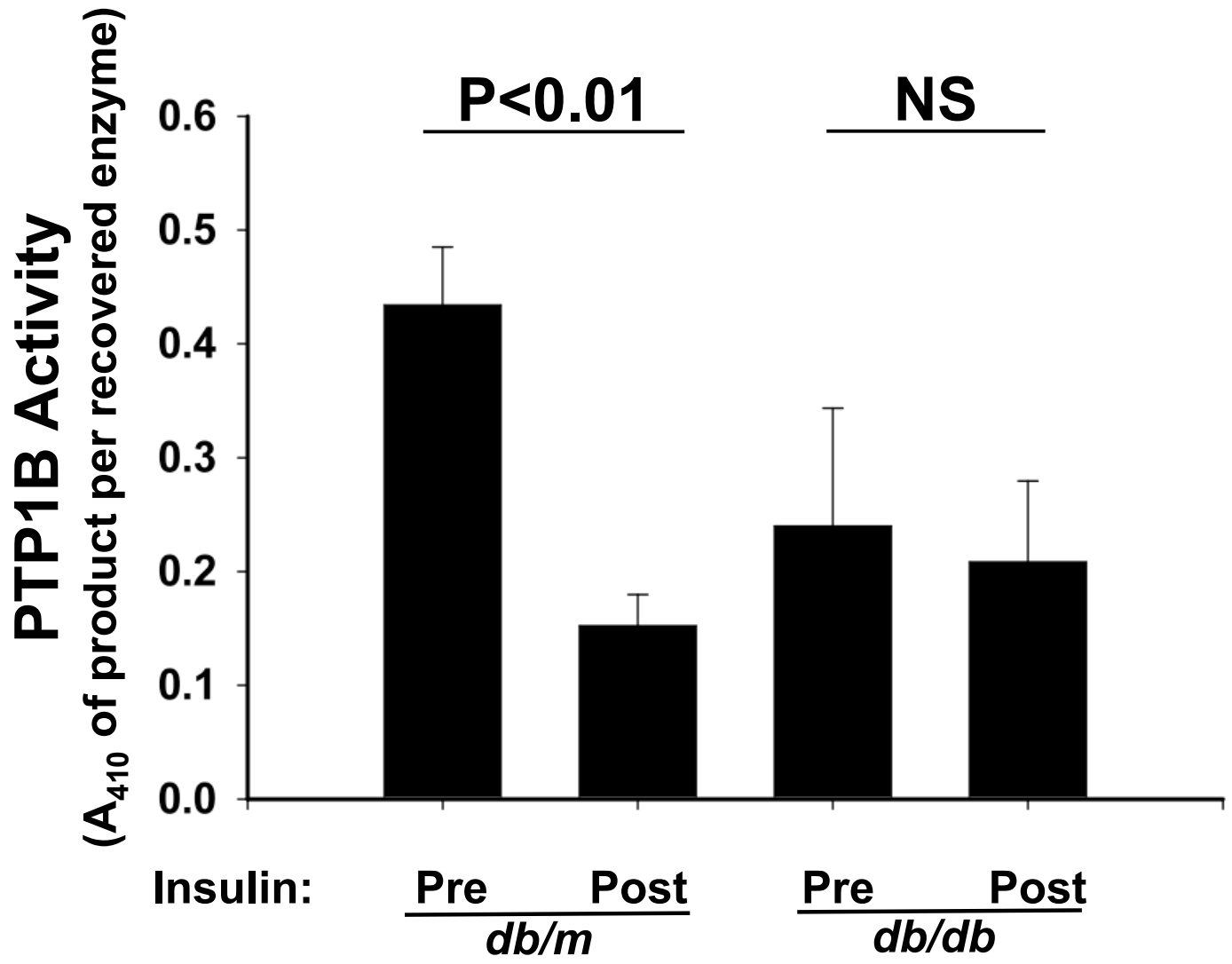

Supplemental Figure II-A,B

II-A

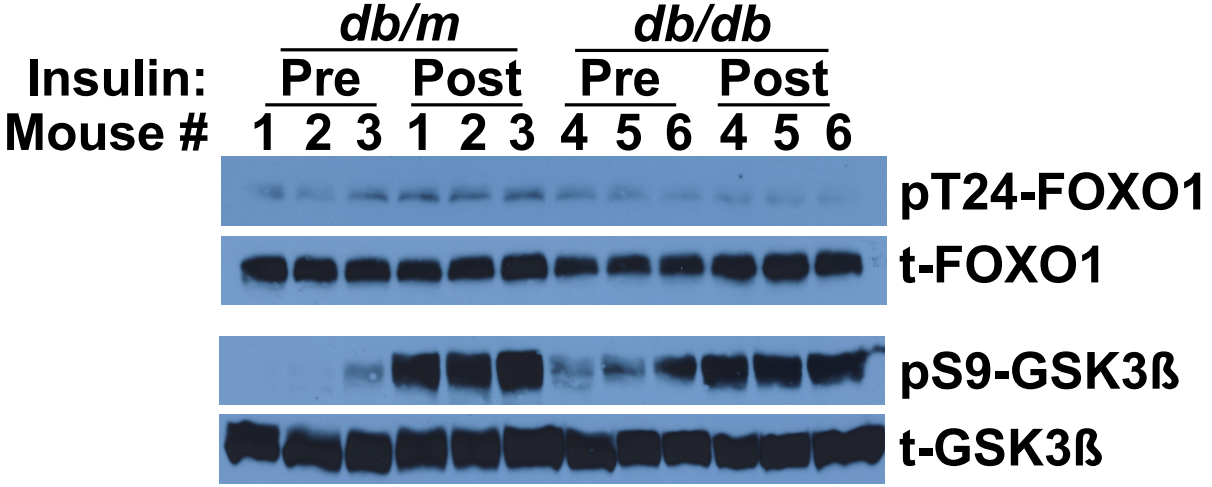

II-B

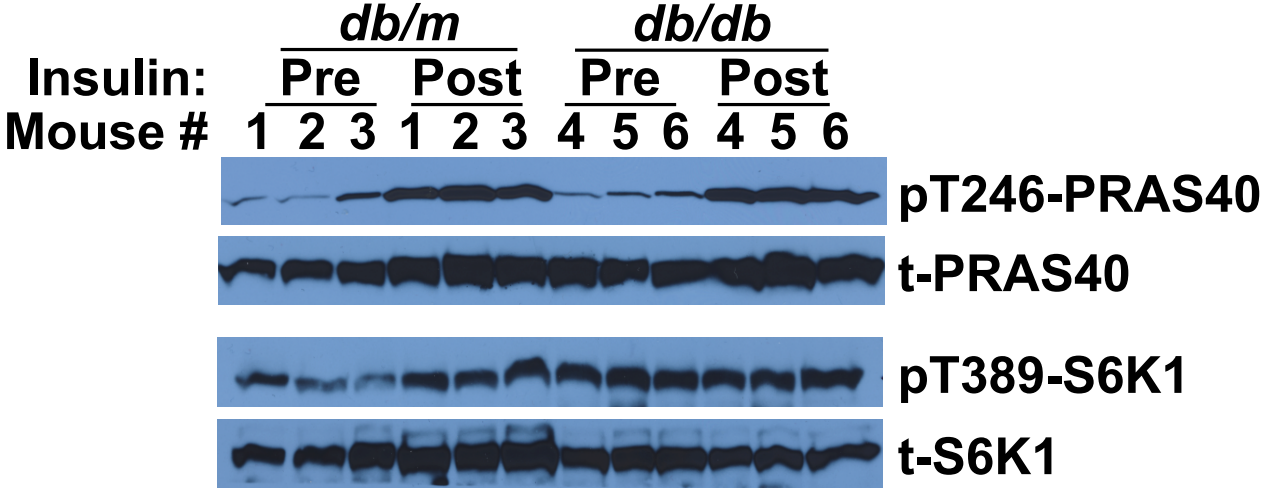

Supplemental Figure II-C

II-C

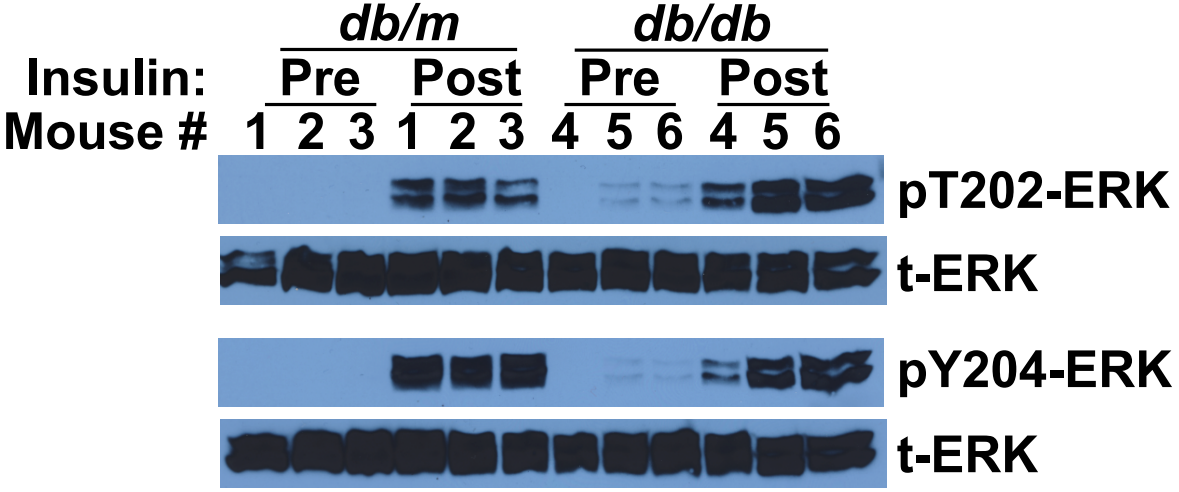

Supplemental Figure III